Competition of coalescence and "fireball" processes in nonequilibrium emission of light charged particles from p + Au collisions

A. Budzanowski,[1] M. Fidelus,[2] D. Filges,[3] F. Goldenbaum,[3] H. Hodde,[4] L. Jarczyk,[2] B. Kamys,[2,*] M. Kistryn,[1] St. Kistryn,[2] St. Kliczewski,[1] A. Kowalczyk,[2] E. Kozik,[1] P. Kulessa,[1,3] H. Machner,[3] A. Magiera,[2] B. Piskor-Ignatowicz,[2,3] K. Pysz,[1,3] Z. Rudy,[2] R. Siudak,[1,3] and M. Wojciechowski[2]
(PISA Collaboration)
[1]*H. Niewodniczański Institute of Nuclear Physics PAN, Radzikowskiego 152, PL-31342 Kraków, Poland*
[2]*M. Smoluchowski Institute of Physics, Jagellonian University, Reymonta 4, PL-30059 Kraków, Poland*
[3]*Institut für Kernphysik, Forschungszentrum Jülich, D-52425 Jülich, Germany*
[4]*Institut für Strahlen- und Kernphysik, Bonn University, D-53121 Bonn, Germany*
(Received 27 November 2007; published 22 August 2008)

The energy and angular dependence of the double differential cross sections $d^2\sigma/d\Omega dE$ were measured for $p, d, t,{}^{3,4,6}$He, ^{6,7,8,9}Li, ^{7,9,10}Be, and ^{10,11,12}B isotopes produced in reactions of 1.2- and 1.9-GeV protons on a Au target. The beam energy dependence of the data, supplemented by the cross sections from a previous experiment at 2.5 GeV, is very smooth. The shape of the spectra and angular distributions do not change significantly in the beam energy range from 1.2 to 2.5 GeV. However, the absolute value of the cross sections increases for all ejectiles. The intermediate mass fragment spectra and their angular distributions are very well reproduced by a phenomenological model of two emitting, moving sources, with parameters smoothly varying with energy. The double differential cross sections for light charged particles were analyzed in the framework of the microscopic model calculations of intranuclear cascade, including the coalescence of nucleons and a statistical model for evaporation of particles from excited residual nuclei. However, the energy and angular dependencies of the data agree with neither predictions of the microscopic intranuclear cascade calculations for protons nor the coalescence calculations for other light charged particles. A very good description of the data is achieved by the phenomenological inclusion of the emission of light charged particles from a "fireball" (i.e., a fast and hot moving source). It was found that the nonequilibrium processes are very important for the production of light charged particles. They exhaust 40%–80% of the total cross section—depending on the emitted particles. Coalescence and fireball emission yield comparable contributions to the cross sections with the exception of the ^{3}He data where coalescence clearly dominates. For all light charged particles, the ratio of nonequilibrium processes to processes proceeding through a phase of statistical equilibrium does not change significantly between the beam energies of 1.2 and 2.5 GeV.

DOI: 10.1103/PhysRevC.78.024603 PACS number(s): 25.40.Sc, 25.40.Ve

I. INTRODUCTION

In a recent publication [1], we have shown inclusive spectra of the double differential cross sections $d^2\sigma/d\Omega dE$ for light charged particles (LCPs) and intermediate mass fragments (IMFs) produced in 2.5-GeV p + Au reactions. The spectra are compatible with the mechanism similar to the cold breakup model proposed by Aichelin *et al.* [2]. According to this model, the proton impinging on the target drills a cylindrical hole in the nucleus, which results in the presence of three sources emitting LCPs, namely a small, fast, and hot "fireball" consisting of several nucleons [3] and two heavier, excited prefragments. They differ significantly in size because the distribution of impact parameters favors noncentral collisions, leading to asymmetric mass values of the products. Therefore, the heavier prefragment is almost indistinguishable from the target residuum, which, according to microscopic models, is created as a result of the intranuclear cascade. The lighter prefragment has typically a mass of about 20–30 nucleons. IMFs, the particles heavier than α particles but lighter than fission fragments, cannot be emitted from the fireball, which consists of only a few nucleons. However, contributions from both heavier prefragments have well been visible in the spectra [1].

This simple picture of the reaction mechanism is very appealing because it offers the opportunity to understand the presence of large nonequilibrium contributions to the experimental cross sections. The contributions cannot quantitatively be reproduced by any of the existing microscopic models based on the assumption of two stages of the reaction. Here, a fast stage consists of the intranuclear cascade of nucleon-nucleon collisions as described by intranuclear cascade (INC), Boltzmann-Uehling-Uhlenbeck, or quantum molecular dynamics models. A slow stage of the reaction in which the heavy target residuum reaches statistical equilibrium and evaporates particles is described by statistical models. It should be pointed out that the phenomenological analysis published in our previous work is indeed unable to unambiguously distinguish between the two processes. A heavy target residuum would be indistinguishable from heavy, excited prefragments from the fast breakup of the target.

*ufkamys@cyf-kr.edu.pl

The need for insight into the reaction mechanism necessitates the investigation of the energy dependence of the reaction processes and the detailed study of the interaction of protons with various targets. The essential goal of the present work is to examine the beam energy dependence of the emission of LCPs and IMFs from the collisions of protons with a Au target in a broad proton energy range, from 1.2 to 2.5 GeV. For this purpose, new experimental data were acquired and analyzed. Where possible, the results are confronted with a microscopic description of the data instead of a purely phenomenological treatment as in Ref. [1].

The experimental data are discussed in Sec. II and the theoretical analysis is described in Sec. III. The obtained results are discussed in the Sec. IV. A summary of the results is provided in the last section.

II. EXPERIMENTAL DATA

The experiment was performed with a self-supporting Au target of thickness 300 μg/cm^2 and the internal proton beam of the COoler SYnchrotron (COSY) at the Jülich Forschungszentrum, Germany. A detailed description of the experimental setup and procedure of data taking is found in Refs. [1] and [4]. Here, we only point out that the operation of the beam was performed by making use of a supercycle in COSY. The supercycle consists of alternating cycles for desirable energies of accelerated protons. During each cycle the protons injected from the cyclotron to the COSY ring were accelerated to the final energy and the beam was steered onto the target. The irradiation time of the target during a given cycle was adjusted to achieve constant reaction rates for all beam energies. All experimental conditions including the setup, the electronics, and the target thickness and its position were exactly the same for the three studied proton energies—1.2, 1.9, and 2.5 GeV. In this way, the energy dependence was not biased by any systematic effects.

Double differential cross sections $d^2\sigma/d\Omega dE$ were measured as a function of scattering angle and energy of ejectiles, which were mass and charge identified for isotopes of H, He, Li, Be, and B. Heavier ejectiles (i.e., C, N, O, F, Ne, Na, Mg, and Al) were identified in terms of their charge only. Typical spectra of isotopically identified ejectiles obtained in the present experiment are shown in Fig. 1. As can be seen in this figure, the shape of the spectra does not vary significantly with beam energy. The essential effect, present for all products, is a monotonic increase of the absolute value of the cross sections with beam energy. Furthermore, all the spectra contain two components: a low-energy component of Gaussian shape, attributed to the evaporation from an equilibrated, excited nucleus, and a high-energy exponential component, interpreted as a contribution of the nonequilibrium mechanism. The data for LCPs, represented in Fig. 1 by α particles, have similar character and energy dependence as those for IMFs.

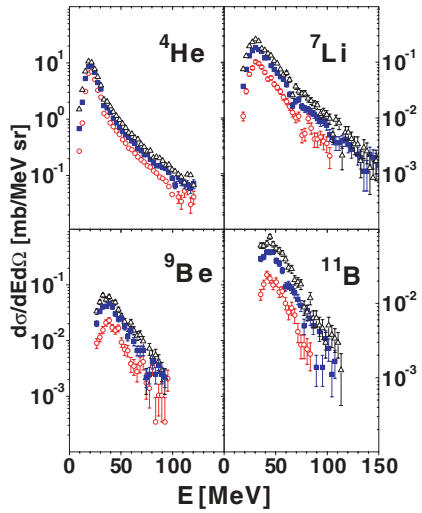

FIG. 1. (Color online) Typical spectra of ^{4}He, ^{7}Li, ^{9}Be, and ^{11}B ejectiles (see legend) measured at 35° for three energies of the proton beam—1.2, 1.9, and 2.5 GeV—impinging onto the Au target. Open circles represent the lowest energy, full squares represent the intermediate energy, and open triangles show the data for the highest energy. The cross sections for the 2.5-GeV proton beam energy were published in Ref. [1] and the data at 1.2 and 1.9 GeV were obtained in the present experiment.

III. THEORETICAL ANALYSIS

The equilibrium emission of LCPs and IMFs may be equally well described by a statistical model of particle evaporation from an excited heavy target residuum created in the fast stage of the reaction. This is, however, not the case for the nonequilibrium emission of composite particles, which cannot be satisfactorily described by models used for reproduction of the first stage of the reaction. Approaches depicting the first stage of the reaction as, for example, intranuclear cascade, Boltzmann-Uehling-Uhlenbeck, or quantum molecular dynamics models generally neglect to a large extent possible multinucleon correlations, which can be crucial for nonequilibrium processes. Whereas it is possible to effectively take these correlations into account for LCPs—by introducing coalescence of emitted nucleons into clusters—such a procedure is insufficient for the description of IMFs nonequilibrium emission. For this reason here a different theoretical analysis has been performed for LCPs and for IMFs.

The IMF data have been analyzed in the frame of a phenomenological model of two moving sources, as was done for the data measured at 2.5-GeV beam energy in the previous investigation of these reactions [1]. Hence the energy dependence of IMF production could be studied in a consistent way. The analysis performed for IMFs is described in Sec. III A. In contrast to the situation for IMFs the nonequilibrium emission of LCPs can be analyzed in the frame of a microscopic model, in which it is assumed that the mechanism of nonequilibrium reactions consists in intranuclear cascade of nucleon-nucleon collisions [5] accompanied by coalescence of the nucleons escaping from the nucleus, as was done in Refs. [6,7]. The authors of these papers claimed that the main properties of nonequilibrium emission of LCPs are well reproduced by the proposed microscopic model. Thus, in the present study the INCL4.3 computer program [7] has been used for the description of the intranuclear cascade of nucleon-nucleon

collisions with inclusion of coalescence of nucleons. For the evaluation of the evaporation of particles from the heavy target residuum remaining after the intranuclear cascade, the GEM2 computer program [8,9] was employed. It was also investigated whether eventual disagreement of the microscopic model calculations with experimental results leaves still room for a contribution from another mechanism, namely the fireball emission postulated in our previous paper [1]. This analysis is described in Sec. III B.

A. Intermediate mass fragments

The main assumptions of the phenomenological model of two moving sources have been formulated in the paper of Westfall *et al.* [10]. They consist in the description of double differential cross sections $d^2\sigma/d\Omega dE$ as incoherent sums of contributions originating from isotropic emission of particles from two sources moving in a direction parallel to the beam direction. Both sources are described by Maxwellian distributions of the energy available for the two body decay resulting in emission of the detected particles. The velocity β of the source, its temperature T, and the contribution to the total production cross section σ are treated as free parameters. The presence of the Coulomb barrier, which hinders the emission of low-energy particles, was originally taken into account by introducing a sharp cutoff for the low energy part of the spectra. To account for the tunneling effect through the barrier as well as for the lack of information on the shape of the barrier the spectra were averaged over uniform or Gaussian probability distributions of the height of the barrier. It was found that the result is not sensitive to details of the assumed distributions. In our recent paper [1] we used another method; namely, we multiplied the Maxwellian energy distribution by a smooth function corresponding to the transmission probability through the barrier. The presence of the Coulomb barrier introduces two parameters that influence mainly the low-energy part of the spectra: (i) the k parameter, which is the height of the Coulomb barrier in units of the height of the barrier B of two charged, touching spheres of radius 1.44 $A^{1/3}$ fm, where $B = Z_1 Z_2 e^2/1.44(A_1^{1/3} + A_2^{1/3})$ MeV, and (ii) the ratio B/d, where d is a diffuseness of the transmission function through the barrier. Then the transmission probability is given by $P(E) = \{1 + \exp[(E - kB)/d)]\}^{-1}$. Details of this procedure along with interpretation of parameters of the model can be found in the appendix of Ref. [1].

The parameters of the two moving sources were fitted to the experimental energy spectra measured at seven angles: 16°, 20°, 35°, 50°, 65°, 80°, and 100°. To decrease the number of parameters it was assumed that the velocity of the slow source emitting IMFs is equal to the velocity of the heavy residuum as calculated by the intranuclear cascade model (i.e., $\beta_1 = 0.003$). A reasonable variation of this velocity influences only very slightly the values of the other parameters (e.g., its modification by 30% causes changes of the other parameters even smaller than the errors estimated by the fitting routine). Furthermore, the B/d ratio was arbitrarily assumed to be equal to 5.5. In the evaluation of the k parameter it was assumed that B is defined as the Coulomb barrier between the emitted particles and the target nucleus. This assumption allows for an easy comparison of the k-parameter values for different ejectiles and emitting sources.

In most cases the computer routine searching for the best-fit values of the parameters was also able to provide estimation of errors of the parameters. However, sometimes an error estimation was not possible, especially when strong ambiguities of parameters were present. Therefore in Table I, some values of the parameters are quoted without the estimation of errors. In this case it may happen that the accuracy of determination of these parameters is poorer than the one for parameters accompanied by estimates of errors.

A very good description of the spectra of all IMFs has been obtained, as can be judged from χ^2 values quoted in Table I, which vary usually between 1 and 2.

As can be seen in Table I, the values of the parameters found from the fit to the data obtained at 1.2 and at 1.9 GeV are very close to those determined in the analysis of the data for 2.5-GeV incident proton beam energy. This is not true for the total cross sections, which increase monotonically with energy for both emitting sources. This increase is illustrated by Fig. 2, where ratios of the total cross sections found for data at 1.2 GeV and at 1.9 GeV to cross sections found for data at 2.5 GeV are shown as open circles and full dots, respectively. The ratios of total cross sections for the fast source are shown in the upper part of the figure and those for the slow source

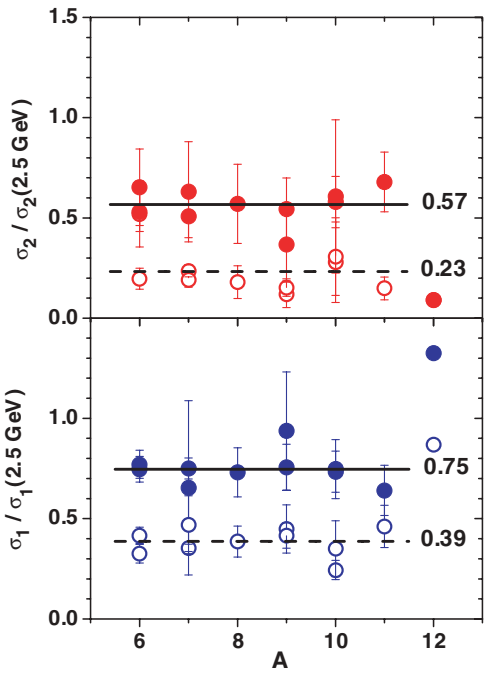

FIG. 2. (Color online) Cross section ratios vs A. The symbols σ_1 and σ_2 correspond to the slow and fast emitting sources, respectively. Full dots represent the ratio of production cross sections of the beam energy of 1.9 GeV to those found at 2.5 GeV as a function of the mass of emitted IMFs. Open circles depict the ratio for cross sections measured at 1.2 GeV to those determined at 2.5 GeV. The lines show the average values of the ratios, 0.23 and 0.57 for the fast source at 1.2 and 1.9 GeV, respectively, as well as 0.39 and 0.75 for the slow source at these energies.

TABLE I. Parameters of two moving sources for isotopically identified IMFs: k, β, T, and σ correspond to the reduced height of the Coulomb barrier for emission of fragments (see the text for explanation), source velocity, its apparent temperature, and total production cross section (integrated over angle and energy of detected particles), respectively. The left part of this Table corresponds to the slow moving source (parameters with indices "1"), while the right part contains values of parameters for the fast moving source. The upper row for each ejectile corresponds to beam energy 1.2 GeV, the intermediate row to 1.9 GeV, and the lowest one to the energy 2.5 GeV. Velocities for the slow sources are fixed at a value of 0.003c estimated as velocities of heavy target residua resulting from intranuclear cascade calculations.

Ejectile	Slow source			Fast source				χ^2
	k_1	T_1 (MeV)	σ_1 (mb)	k_2	β_2	T_2 (MeV)	σ_2 (mb)	
^{6}He	0.97 ± 0.09	9.3 ± 1.1	8.1 ± 1.1	0.47 ± 0.05	0.034 ± 0.007	13.6 ± 1.2	3.9 ± 1.0	2.7
	0.95 ± 0.04	9.1 ± 0.6	18.5 ± 1.2	0.36 ± 0.05	0.040 ± 0.007	19.1 ± 1.3	4.9 ± 1.1	2.6
	0.97 ± 0.04	9.0 ± 0.6	24.8 ± 1.4	0.35 ± 0.05	0.040 ± 0.007	21.6 ± 1.4	7.5 ± 1.4	2.1
^{6}Li	0.89 ± 0.05	12.4 ± 0.9	10.5 ± 0.8	0.43 ± 0.08	0.047 ± 0.008	22.2 ± 1.3	2.9 ± 1.3	2.4
	0.85 ± 0.04	12.1 ± 0.7	19.5 ± 1.2	0.43 ± 0.05	0.040 ± 0.004	23.6 ± 0.7	7.7 ± 1.1	2.4
	0.86 ± 0.04	11.1 ± 0.8	25.3 ± 1.7	0.44 ± 0.04	0.034 ± 0.003	23.7 ± 0.6	14.5 ± 1.7	2.0
^{7}Li	0.89	12.3	18.0	0.47	0.039	16.4	4.8	4.7
	0.88 ± 0.03	11.7 ± 0.5	38.1 ± 1.8	0.37 ± 0.04	0.040 ± 0.005	20.3 ± 0.7	10.3 ± 1.7	4.2
	0.88 ± 0.03	11.6 ± 0.6	50.8 ± 2.6	0.36 ± 0.03	0.035 ± 0.003	20.9 ± 0.5	20.3 ± 2.6	3.1
^{8}Li	0.94 ± 0.11	11.1 ± 1.6	3.51 ± 0.45	0.48 ± 0.08	0.040 ± 0.008	14.4 ± 2.0	1.15 ± 0.45	1.8
	0.90 ± 0.08	11.8 ± 1.3	6.65 ± 0.90	0.43 ± 0.05	0.032 ± 0.006	17.2 ± 1.1	3.65 ± 0.93	2.5
	0.90 ± 0.09	11.9 ± 1.5	9.1 ± 1.4	0.45 ± 0.05	0.029 ± 0.005	18.0 ± 1.0	6.4 ± 1.5	2.1
^{9}Li	1.01 ± 0.19	11.9 ± 2.9	0.92 ± 0.09	0.58 ± 0.33	0.044 ± 0.008	4.1 ± 1.8	0.25 ± 0.12	1.1
	0.84 ± 0.09	10.4 ± 3.0	1.92 ± 0.37	0.51 ± 0.08	0.034 ± 0.008	11.9 ± 2.5	0.77 ± 0.33	1.5
	1.00 ± 0.22	10.4 ± 3.0	2.1 ± 0.5	0.39 ± 0.07	0.025 ± 0.003	18.2 ± 1.6	2.1 ± 0.6	1.2
^{7}Be	0.89	13.3	1.22	0.52	0.036	25.3	0.88	1.1
	0.86 ± 0.21	14.1 ± 5.3	1.7 ± 1.0	0.61 ± 0.06	0.025 ± 0.007	22.8 ± 1.2	2.9 ± 1.0	1.2
	0.92 ± 0.27	11.2 ± 4.3	2.6 ± 0.8	0.48 ± 0.05	0.038 ± 0.005	24.0 ± 1.2	4.6 ± 0.9	1.4
^{9}Be	0.86	9.7	5.2	0.50	0.030	15.2	1.24	1.7
	0.88	9.8	9.5	0.59	0.022	15.0	4.41	1.4
	0.86 ± 0.12	9.6 ± 1.7	12.5 ± 1.9	0.53 ± 0.06	0.020 ± 0.005	16.6 ± 0.8	8.1 ± 2.3	1.4
^{10}Be	0.86 ± 0.16	12.4 ± 2.1	3.5 ± 1.3	0.62 ± 0.14	0.024 ± 0.011	9.0 ± 3.7	1.9 ± 1.3	1.8
	0.86	12.0	7.34	0.47	0.027	13.3	3.94	1.8
	0.90 ± 0.08	11.8 ± 1.2	10.0 ± 1.4	0.44 ± 0.04	0.026 ± 0.004	14.5 ± 0.9	6.8 ± 1.5	1.3
^{10}B	0.83	11.7	1.61	0.78	0.017	15.9	0.83	2.8
	0.87	10.2	4.93	0.70	0.021	17.7	1.64	1.5
	0.85 ± 0.20	10.5 ± 3.4	6.6 ± 1.3	0.73 ± 0.14	0.020 ± 0.010	18.2 ± 2.7	2.7 ± 1.7	1.8
^{11}B	0.84 ± 0.11	10.6 ± 1.4	5.9 ± 0.7	0.53 ± 0.08	0.032 ± 0.008	10.6 ± 2.2	1.9 ± 0.6	0.94
	0.90	10.2	8.2	0.57	0.019	13.9	8.7	1.6
	0.93 ± 0.18	10.5 ± 2.1	12.8 ± 2.5	0.50 ± 0.05	0.022 ± 0.004	14.5 ± 0.7	12.8 ± 2.8	1.7
^{12}B	0.83	11.9	1.39	0.54	[0.032]	12.5	0.46	1.3
	0.88	7.8	2.12	0.71	0.017	13.5	2.57	1.2
	0.87	8.8	1.6	0.73	0.012	13.2	5.1	1.0

are depicted in the lower part. The following conclusions can be derived from inspection of Fig. 2:

(i) The ratios of the cross sections for both sources, $\sigma_1(E, A)/\sigma_1(2.5\ \text{GeV}, A)$ and $\sigma_2(E, A)/\sigma_2(2.5\ \text{GeV}, A)$, are independent of the mass A of ejectiles (with the exception of the ^{12}B cross sections, which are, however, not well determined because of poor statistics of the data).

(ii) The cross sections for both sources are always larger for $E = 1.9$ GeV than the cross sections for $E = 1.2$ GeV (full dots are above open circles) and the cross sections for $E = 2.5$ GeV are the largest (the ratios are always smaller than unity).

(iii) The ejectile ratios averaged over mass of the cross sections for the slow source, $\langle\sigma_1(1.2\ \text{GeV})/\sigma_1(2.5\ \text{GeV})\rangle = 0.39$ and $\langle\sigma_1(1.9\ \text{GeV})/\sigma_1(2.5\ \text{GeV})\rangle = 0.75$, are larger than the corresponding ratios for the fast source, $\langle\sigma_2(1.2\ \text{GeV})/\sigma_2(2.5\ \text{GeV})\rangle = 0.23$ and $\langle\sigma_2(1.9\ \text{GeV})/\sigma_2(2.5\ \text{GeV})\rangle = 0.57$. This means that the cross sections of the slow source increase relatively slower in the beam energy range from 1.2 to 2.5 GeV than the cross sections attributed to the fast source; thus the contribution from the fast source becomes more important for higher beam energies. This is confirmed by the fact that the relative contribution $\sigma_2(E, A)/[\sigma_1(E, A) + \sigma_2(E, A)]$ of the fast source to the total production cross section of IMFs, evaluated using the numbers from Table I, increases with energy in almost the same way for all IMFs. On average this contribution is equal to 0.27 ± 0.03, 0.33 ± 0.05, and 0.44 ± 0.05

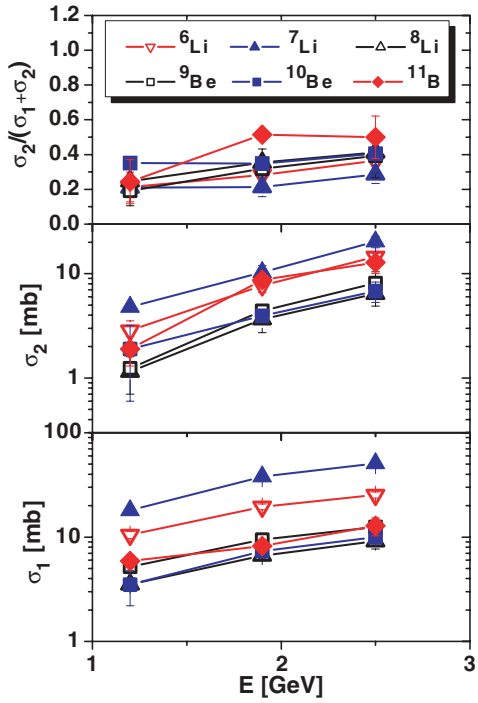

FIG. 3. (Color online) Energy dependence of the cross section σ_1, corresponding to the emission from the slow source (lower panel), energy dependence of the cross section σ_2, related to emission from the fast source (middle panel), and energy dependence of the relative contribution of the fast source (upper panel).

for beam energies equal to 1.2, 1.9, and 2.5 GeV, respectively.

These findings are also illustrated by Fig. 3, in which the energy dependence of cross sections σ_1 and σ_2 is shown for the emission from the slow and fast sources, respectively, as well as the energy dependence of the relative contribution of the fast source σ_2 to the total cross section $\sigma_1 + \sigma_2$. Note the utilization of different scales in Fig. 3 (linear for the upper part of the figure and logarithmic for the middle and lower parts). It may be observed that σ_1 and σ_2 vary rather rapidly with energy, σ_1 increases by a factor of ~2–3 in the energy range studied, and σ_2 increases even more (i.e., by a factor of ~3–5). However, the relative contribution of the nonequilibrium mechanism, that is, $\sigma_2/(\sigma_1 + \sigma_2)$, increases much more slowly, as was previously mentioned, because of the same energy trend for both cross sections σ_1 and σ_2.

B. Light charged particles

It is well known that the cross sections for the production of LCPs are at least an order of magnitude larger than those for the emission of IMFs. Therefore, knowledge of the mechanism of LCP production is crucial for understanding the full interaction process. The coalescence mechanism seems to be very promising for a possible explanation of the nonequilibrium production of LCPs [6,7]. However, it is obvious that such a hypothesis relies on the proper reproduction of the nucleon spectra by the intranuclear cascade mechanism. The lack of a good description of the proton spectra by exclusively applying the coalescence mechanism for the nonequilibrium emission of LCPs calls for an additional reaction mechanism to come into play. To study the importance of the coalescence in the production of LCPs, the experimental proton spectra for the three energies under consideration were compared with predictions of the intranuclear cascade model coupled with the evaporation of nucleons. The calculations have been performed by means of the INCL4.3 computer program [7] in which the coalescence of nucleons can optionally be taken into account, whereas the evaporation of protons as well as complex particles was described by the GEM2 computer model [8,9].

Such calculations, done with and without inclusion of the coalescence mechanism, are presented in Fig. 4 as dashed and solid lines, respectively, together with the experimental proton spectra, shown as circles.

As can be seen, the theoretical spectra obtained from calculations neglecting the coalescence overestimate the experimental spectra for proton beam energy of 1.2 GeV, but they underestimate a big part of the spectra at beam energy of 2.5 GeV, in particular for most forward angles. It seems that the

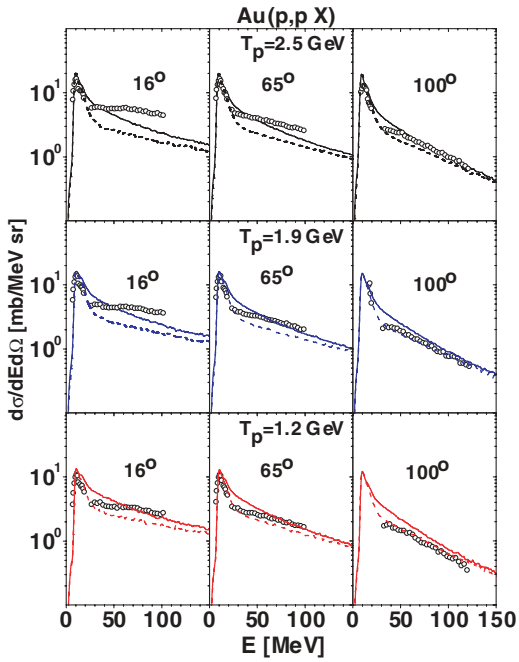

FIG. 4. (Color online) Double differential cross sections as a function of energy. Open circles represent experimental energy spectra of protons measured at selected angles—16°, 65°, and 100° (left, central, and right columns of the figure, respectively)—for proton beam energies of 1.2 and 1.9 GeV from the present experiment and 2.5 GeV from Ref. [1] (lower, central, and upper rows of the figure, respectively). The solid lines show the results of calculations performed in the frame of the intranuclear cascade formalism by means of the INCL4.3 program [7] combined with the evaporation of protons from an excited residual nucleus after the fast stage of the reaction evaluated by means of the GEM2 model [8,9]. The dashed lines present calculations also performed with INCL4.3 plus GEM2 programs; however, the coalescence of nucleons into light complex particles is taken into account according to the prescription proposed in Ref. [7].

TABLE II. Parameters of the fireball: β, T, and σ, corresponding to the fireball velocity, its apparent temperature, and the total production cross section (integrated over angle and energy of detected particles), respectively. B/d determines the ratio of the threshold energy for the emission of the particles (height of the Coulomb barrier) to diffuseness of the transmission function through the barrier. The parameter F is the scaling factor of the coalescence and evaporation contribution extracted from a fit to the proton spectra. The numbers in brackets show fixed values of the parameters. Note that for α particles an additional moving source should be added with parameters given in Table III.

E_p (GeV)	Ejectile	β	T (MeV)	σ (mb)	B/d	F	χ^2
1.2	p	0.136	36.7	1400	11.4	0.63	27.2
	d	0.160	39.1	190	12.1	[0.63]	9.5
	t	0.073	21.5	87	4.5	[0.63]	2.9
	^{3}He	[0.073]	[21.5]	0.44	18	[0.63]	4.5
	^{4}He	0.070	19.0	49	6.2	[0.63]	13.5
1.9	p	0.160	40.7	1950	11.9	0.69	46.5
	d	0.155	41.1	330	19.0	[0.69]	15.3
	t	0.066	23.8	170	3.1	[0.69]	4.4
	^{3}He	0.045	15.0	15.6	5.2	[0.69]	3.3
	^{4}He	0.061	20.9	110	4.7	[0.69]	15.1
2.5	p	0.156	41.7	2720	12.0	0.73	39.0
	d	0.130	42.3	530	8.6	[0.73]	10.5
	t	0.050	23.3	300	5.7	[0.73]	3.2
	^{3}He	0.037	20.5	54	5.8	[0.73]	2.7
	^{4}He	0.051	20.7	210	3.7	[0.73]	11.5

theoretical proton spectra evaluated without coalescence have different beam energy dependence compared to the experimental data. The inclusion of coalescence significantly decreases the theoretical cross sections for protons, in particular between 40- and 100-MeV kinetic energy. It is observed that theoretical spectra are below the experimental data for all beam energies and for all scattering angles. The height of the evaporation peak is slightly overestimated in both options of the calculations.

Further inspection of Fig. 4 leads to the conclusion that there are two obvious trends in the difference of the theoretical spectra evaluated with the coalescence mechanism and the experimental data: (i) The higher the beam energy, the larger the underestimation of the high-energy part of the data by theory and (ii) the smaller the scattering angle with respect to the proton beam direction, the larger the underestimation of the experimental data. These effects might be explained by assuming the presence of an additional process, which manifests itself mainly at small scattering angles and gives increasing contribution to the emission of protons for larger beam energies. Such a contribution can correspond to the presence of the fireball emission, which owing to fast motion in the forward direction should modify the cross sections mainly at forward scattering angles. However, in the microscopic calculations performed according to the intranuclear cascade model there is no explicit room for such a process. Therefore, the inclusion of a fireball emission should consequently be accompanied by decreasing the contribution from the direct processes simulated by intranuclear cascade and coalescence of escaping nucleons. According to this reasoning, the spectra of protons evaluated from the intranuclear cascade with inclusion of coalescence added to the contribution of evaporated protons were multiplied by a factor $\leqslant 1$. This factor is common for all scattering angles and treated as a free parameter of the fit. The scaled intranuclear cascade and evaporation contribution of protons is added to the contribution from the fireball emission calculated according to the formula of a single moving source emitting the LCPs isotropically [10]. The parameters of the single moving source (the fireball), that is, its temperature parameter T, its velocity β, and the total production cross section associated with this mechanism, σ, were also treated as free parameters. The height of the Coulomb barrier between the fireball and the emitted ejectile was arbitrarily fixed at 2% of the estimated Coulomb barrier for the emission from the target nucleus. The values of the parameters associated with the fireball are given in Table II.

The fit was performed for seven scattering angles (16°, 20°, 35°, 50°, 65°, 80°, and 100°). The results of the fit are presented in Fig. 5 for three angles, the smallest, the intermediate, and the largest, where the dashed lines show the contribution of intranuclear cascade with surface coalescence and evaporation, the dash-dotted lines present contribution from the fireball emission, and the solid line depicts the sum of all contributions. As can be seen, an excellent agreement could be obtained for all scattering angles and beam energies. It is worth emphasizing that the fireball contribution to the spectra increases significantly, not only with the decrease of the scattering angle but also with the increase of the beam energy.

The success in describing the proton spectra by the microscopic model of intranuclear cascade with coalescence of nucleons and evaporation of protons from equilibrated target residuum combined with the phenomenological contribution from the fireball emission indicates that the same method of data description might be applicable for other LCPs.

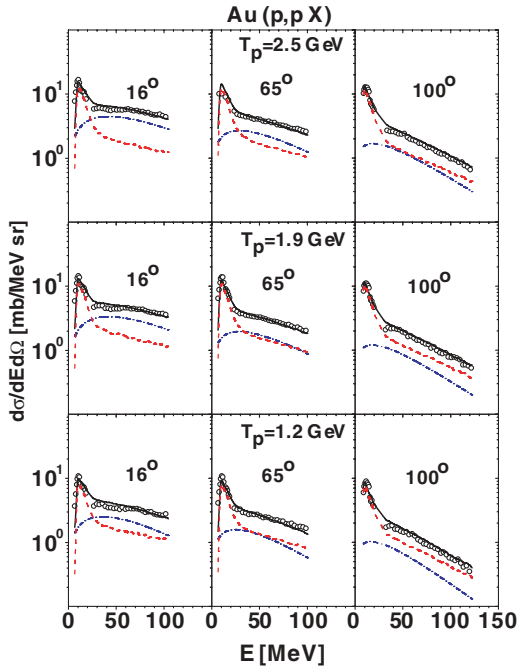

FIG. 5. (Color online) Double differential cross sections as a function of energy. Open circles represent the experimental energy spectra of protons measured at selected angles—16°, 65°, and 100° (left, central, and right columns of the figure, respectively) for proton beam energies of 1.2 and 1.9 GeV from the present experiment and 2.5 GeV from Ref. [1] (lower, central, and upper rows of the figure, respectively). The dot-dashed lines present the contribution of proton emission from the fireball and the dashed lines show calculations performed with INCL4.3 plus GEM2 programs. The INCL4.3 plus GEM2 contributions are scaled by the factors 0.63, 0.69, and 0.73 for beam energies 1.2, 1.9, and 2.5 GeV, respectively. The solid lines show the sum of all these contributions.

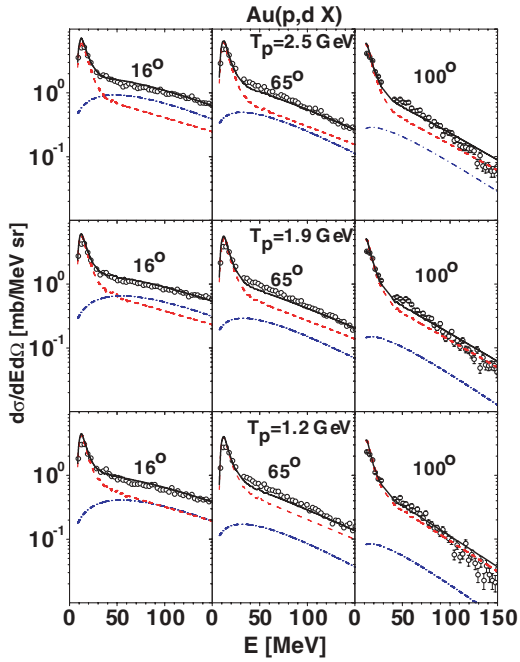

FIG. 6. (Color online) Same as Fig. 5, but for deuterons.

It is natural and justified to scale the model coalescence contribution to spectra of complex LCPs by the very same factor F that was used for the proton spectra because the coalescence emission of complex particles is determined by the yield of nucleons leaving the nucleus after the intranuclear cascade of collisions.

The procedure of fitting parameters characterizing the fireball contribution to the experimental spectra of deuterons, tritons, ^{3}He, and ^{4}He was therefore performed with the same scaling factors of the coalescence and evaporation emission as those for the proton spectra: 0.63, 0.69, and 0.73 for beam energies of 1.2, 1.9, and 2.5 GeV, respectively. A very good description of the experimental data was achieved for all particles with the exception of α particles. For α particles it was necessary to add a contribution of another moving source, one with parameters very close to those used for IMFs. This additional contribution led to a perfect description of the α-particle spectra. The quality of the data reproduction is illustrated by Figs. 6, 7, 8, and 9 for deuterons, tritons, ^{3}He, and ^{4}He, respectively. The parameters of the fireball source are listed in Table II and the parameters of the additional source used for α particles are listed in Table III. As can be seen from the figures, the spectra of deuterons and tritons could not even qualitatively be described by coalescence and evaporation of particles alone. The reason of this is the difference between angular variation of the experimental spectra and those evaluated from the microscopic model. For example, multiplication of the coalescence contribution by a factor that will well reproduce the spectrum at 100°

TABLE III. Parameters of the intermediate mass source needed to describe the α-particle spectra by combination of microscopic model coalescence and evaporation contributions and the fireball and intermediate mass source contributions. Parameters β, T, and σ have the same meaning as for Table II. The k parameter is the height of the Coulomb barrier in units of a simple barrier height estimation by the Coulomb potential of two uniformly touching spheres with the charge of the target nucleus and the charge of the emitted particle with radii parametrized as $R = 1.44A^{1/3}$.

E_p (GeV)	k	β	T (MeV)	σ (mb)
1.2	[0.8]	0.0094	10.6	385
1.9	0.83 ± 0.03	0.0062 ± 0.0010	10.2 ± 0.3	577 ± 23
2.5	0.80 ± 0.04	0.0047 ± 0.0011	10.2 ± 0.4	764 ± 38

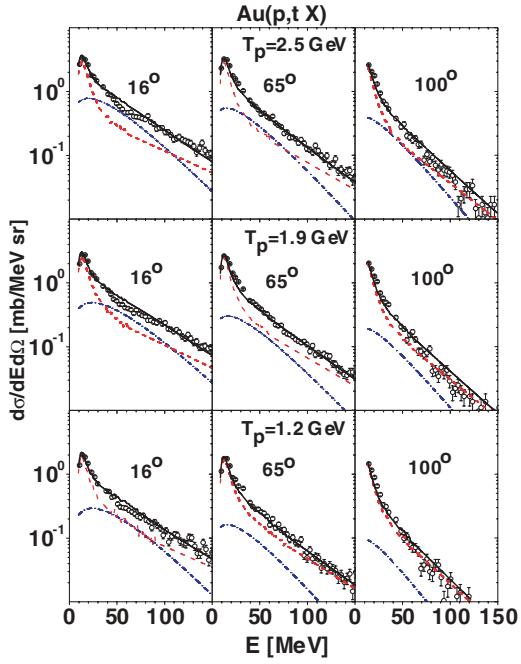

FIG. 7. (Color online) Same as Fig. 5, but for tritons.

still leads to underestimation of the cross sections at smaller angles. In contrast, adding the contribution of emission of deuterons and tritons from the fireball mechanism improves the description significantly because this contribution has exactly such an angular and energy dependence that when added to the microscopic model spectra ensures reproduction of the experimental data.

A different situation is present for the ^{3}He channel, where the fireball contribution seems to be almost negligible, especially at lower beam energies. This means that the

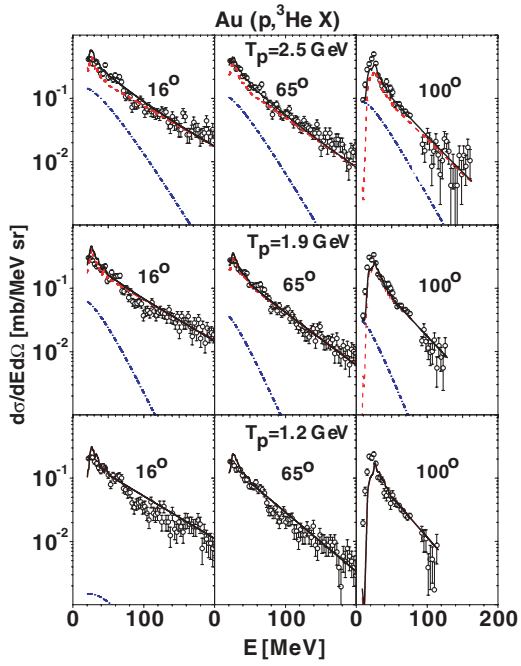

FIG. 8. (Color online) Same as Fig. 5, but for ^{3}He.

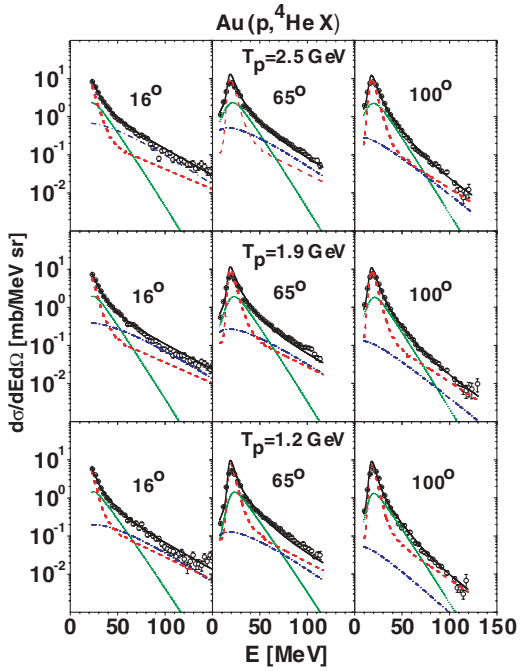

FIG. 9. (Color online) Same as Fig. 5, but for α particles. The thin dotted line depicts the contribution from a fast moving source of a mass intermediate between the fireball and the heavy target residuum.

coalescence together with the small evaporation contribution exhausts almost fully the experimental yield of particles, leaving no room for the fireball emission. It should be, however, emphasized that this very good data reproduction by the coalescence and evaporation mechanisms was obtained after scaling of the theoretical cross sections from INCL4.3 plus GEM2 by the same factors as those used for the theoretical cross sections for proton emission; thus the presence of fireball emission influences also indirectly the description of ^{3}He emission.

Still another reaction mechanism seems to be responsible for the α-particle production. The shape as well as the magnitude of the experimental spectra for ^{3}He and ^{4}He is quite different, showing that the evaporation of α particles from an excited target residuum after the intranuclear cascade of nucleon-nucleon collisions is much higher than the corresponding evaporation of ^{3}He particles. However, the peak present in the experimental spectra of ^{4}He is much broader than that predicted by evaporation from a heavy target residuum. Since neither the coalescence mechanism nor the fireball emission can produce such a peak in the spectrum, another contribution is necessary to reproduce the shape of the peak in the experimental spectra. The naturally appearing solution is to take into consideration the contribution from the moving source of the mass larger than the fireball but smaller than the heavy target residuum. Such a source, moving faster than the target residuum but slower than the fireball, was observed in the analysis of spectra for all IMFs; thus it is not astonishing that also α-particle spectra are modified by its contribution.

IV. DISCUSSION

The temperature of the fireball fitted to describe LCP data varies only slightly with beam energy. Its values listed in Table II do not change by more than ∼10% for each ejectile in the beam energy range from 1.2 to 2.5 GeV. This is also true for the temperature of the additional source needed for a good description of the α-particle data and for temperatures of both phenomenological sources applied for the parametrization of IMF data. This fact allows us to study the dependence of the beam-energy-averaged temperature on the ejectile mass instead of temperature dependencies for individual beam energies. Temperatures averaged over the beam energies of all moving sources are depicted in the lower part of Fig. 10 as a function of the ejectile mass A. It is seen that the temperatures of the two sources emitting IMFs are grouped into two sets: slow sources, which lie along the solid horizontal line $T = 11.1$ MeV, and fast sources, which are spread around the dashed line $T = 30.6–1.61A$ MeV. The same procedure applied to the apparent temperatures of the fireball emitting LCPs shows that the mass dependence of this temperature may be described by a linear function: $T = 49.9–8.24A$ MeV (see dash dotted line in Fig. 10).

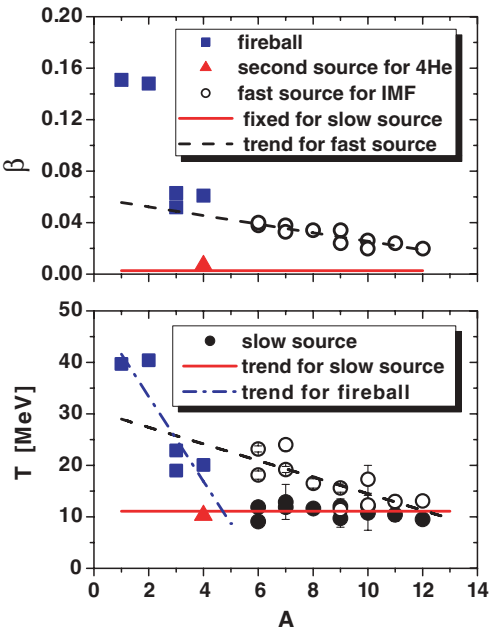

FIG. 10. (Color online) Lower panel: Apparent temperature of the moving sources, averaged over beam energies, as a function of the ejectile mass. Open circles and full dots represent values of parameters obtained from the analysis of IMF data for fast and slow sources, respectively. Full squares depict the temperature of the fireball fitted to spectra of LCPs together with the contribution of the microscopic model of intranuclear cascade, coalescence of nucleons, and statistical evaporation. The full triangle shows the temperature of the second source fitted to spectra of α particles. The solid and dashed lines were fitted to the points representing IMFs and extrapolated to smaller masses. The dash dotted line was fitted to LCP temperatures of the fireball. Upper panel: Dependence of the beam-energy-averaged velocity of the sources vs mass of the ejectiles. The symbols have the same meaning as for the lower part of the figure with one exception: The full dots are not shown because the velocity of the slower source was fixed during the analysis (see text) and it is represented by a solid line in the figure. The dashed line was fitted to the open circles representing velocities of fast source for IMFs. The line was extrapolated to the lower mass region.

If the dependence of the apparent temperature T of the source on the ejectile mass A is caused only by recoil of the source during the emission of registered ejectiles then it is possible to estimate the mass of the source, A_S, and its true temperature τ from the parameters of the linear dependence $T(A)$. For the fast source emitting IMFs the source temperature is equal to $\tau = 30.6$ MeV and its mass is equal to $A_S = 30.6/1.61 \equiv 19$ nucleons. The temperature of the slow source is independent of the IMF mass, which means that the recoil effect is negligible [i.e., the source is very heavy and its temperature is equal to the apparent temperature found in the fit ($\tau = 11.1$ MeV)]. The temperature of the fireball extracted from the parameters of the fitted straight line, analogously to the method used for the fast source, is equal to $\tau = 49.9$ MeV and the fireball is built of $A_S = 49.9/8.24 \equiv 6$ nucleons.

These conclusions seem to be compatible with the results of a pure phenomenological analysis of two moving sources performed in our previous investigation of LCPs and IMFs for p + Au collisions at a proton beam energy of 2.5 GeV [1]. In this study the temperature of the slow source for IMFs was ∼12 MeV, the temperature of the fast source for IMFs was ∼33 MeV, and the temperature of the fireball was estimated to be ∼62 MeV. The mass of the slow source must be very large—close to the mass of the target—because the apparent temperature of this source did not vary significantly with the product mass (i.e., the recoil could be neglected. The mass of the fast source was equal to the mass of ∼20 nucleons and the mass of the fireball was close to the mass of ∼8 nucleons.

The largest deviation between the previous results and those found in the present work concerns the properties of the fireball. This is not surprising because the fireball of the present work is responsible only for a part of the effect that was attributed to the fireball in the previous study. However, inspection of Fig. 10 shows another effect: The straight dashed line representing the apparent temperature of the fast source with the mass of about 19 nucleons—found from analysis of IMFs data—crosses the dash dotted line representing the apparent temperature of the fireball at an ejectile mass of $A \sim 3$. In conclusion, the temperature parameter of the fireball and of the intermediate mass source are the same for tritons, ^{3}He, and ^{4}He. Moreover, the velocity of the fireball that emits tritons, ^{3}He, and ^{4}He is very close to the velocity of the fast source emitting IMFs, as is shown in the upper part of Fig. 10. In this figure the beam-energy-averaged values of the velocity parameter are collected. The velocities of the fast and the slow sources emitting IMFs are represented by open circles and the horizontal line, respectively. The slow source velocity was fixed at the velocity of the heavy residuum as calculated by the intranuclear cascade model. The velocities of the fireballs emitting LCPs are shown as full squares, and the velocity of the additional source, necessary for description of the α particles, is depicted as a full triangle. The similarity of the velocities of the fireball and the fast source of IMFs makes arguable

TABLE IV. Cross sections (in millibarns) for the production of LCPs by the intranuclear cascade and coalescence mechanism (left part of the table) and by evaporation (right part of the table), evaluated with INCL4.3 plus GEM2 computer programs and scaled by appropriate factors: 0.63, 0.69, and 0.73 for beam energies of 1.2, 1.9, and 2.5 GeV, respectively.

E_p (GeV)	Coalescence					Evaporation				
	p	d	t	^{3}He	^{4}He	p	d	t	^{3}He	^{4}He
1.2	2213	613	198	75	62	633	272	134	10.2	718
1.9	2740	771	254	101	80	932	432	212	20.4	914
2.5	3084	859	285	116	90	1094	526	257	27.1	1019

whether one can extract the mass of the fireball from the mass dependence of the apparent temperature of the source fitted to the proton, deuteron, triton, and ^{3,4}He data or whether it is necessary to assume that the source for particles with mass 3 and 4 is identical with the intermediate mass source ($A_S \sim 19$) found for IMFs. If this is the case, then the genuine fireball contributes mainly to emission of protons and deuterons; thus it is reasonable to conjecture that the mass of the fireball should be very light (3–4 nucleons).

It is worth pointing out that the values of the temperature and the velocity of the additional source introduced to describe the α-particle emission (triangles in Fig. 10) are very similar to the values characterizing the slow, heavy source emitting the IMFs (solid line in Fig. 10).

All these findings agree well with conclusions derived from a pure phenomenological analysis of the $p + \mathrm{Au}$ data measured at 2.5-GeV proton beam energy [1]: that the nonequilibrium contribution to the production of LCPs and IMFs indicates the presence of a mechanism similar to the fast breakup of a target nucleus in which three moving sources of ejectiles are created. The new and crucial result of the present work is the observation that the nonequilibrium emission of LCPs is mediated by two competing mechanisms: a surface coalescence of outgoing nucleons and a contribution from three moving sources appearing as result of the breakup.

It is interesting to compare the cross sections for inclusive LCP production originating from these two nonequilibrium mechanisms. The values of cross sections for the nonequilibrium processes are listed in Tables II, III and IV for the emission from the fireball, for the emission from an additional, slower source, and from coalescence, respectively. The proton beam energy dependence of these cross sections and the dependence of the relative contribution of the fireball emission are presented in Fig. 11. Several important conclusions can be derived from the inspection of the figure:

(i) The cross sections for all emitted LCPs increase roughly exponentially with beam energy. However, this increase is faster for the fireball emission (central part of the figure) than for the coalescence mechanism (lower part of the figure).

(ii) The magnitude of the coalescence cross sections decreases strongly with the mass of the ejectile. This behavior may be explained by the decreasing probability of a potential capture of more and more nucleons forming composite particles by the nucleons escaping from the nucleus.

(iii) The cross sections for the two isobars, triton and ^{3}He, are quite different. The cross section for triton production is approximately twice that for ^{3}He. Such a big difference may be related to the ratio $N/Z = 1.49$ of Au nuclei and may be additionally enhanced by the fact that coalescence of two neutral particles (neutrons) and one charged particle (proton) is not influenced by the repulsive Coulomb force, whereas the coalescence of two protons and one neutron is certainly hindered to some extent by the Coulomb interaction. This effect is also visible for the fireball emission of tritons and ^{3}He; moreover, the ratio of the triton cross section to ^{3}He cross sections is larger than for the coalescence and varies (decreases) strongly with beam energy (cf. central part of Fig. 11).

(iv) The relative contribution of the fireball mechanism increases almost exponentially with the beam energy (cf. upper part of Fig. 11). The slope of the energy

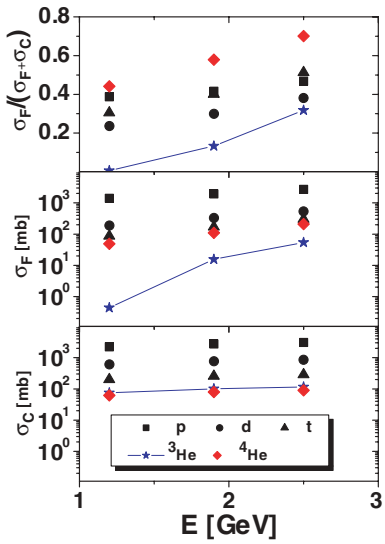

FIG. 11. (Color online) Beam energy dependence of the relative contribution of fireball emission to the whole nonequilibrium production cross sections (upper panel). Energy dependence of the cross section resulting from the fireball mechanism (middle panel). Energy dependence of the production cross sections resulting from coalescence (lower panel). Full squares, dots, and triangles represent proton, deuteron, and triton cross sections, respectively. The stars connected by a solid line show cross sections for ^{3}He production and the diamonds correspond to α-particle cross sections.

dependence is smallest for protons, has an intermediate value for deuterons and tritons, and is largest for ^{3}He and α particles. It should be, however, pointed out that in spite of such a large increase of fireball emission for both helium isotopes, the contribution of this mechanism is less important for these particles than for the hydrogen isotopes. For ^{3}He this is caused by the fact that the relative contribution of the fireball emission is small (being smaller than 20% of the sum of both considered mechanisms) and, furthermore, it manifests itself only at forward angles and small energies (cf. Fig. 8). Thus, ^{3}He spectra can be quite well reproduced by the scaled coalescence mechanism contribution alone. For the α particles, the fireball contribution is comparable to that of the coalescence mechanism; however, as was already discussed, another nonequilibrium process gives a large contribution to the experimental spectra: emission from a source of mass intermediate between that of the fireball and of the heavy target residuum created in the fast stage of the reaction.

The present investigations revealed beam energy variation of the contribution of nonequilibrium processes to the total abundance of studied LCPs. The nonequilibrium processes consist of the fireball emission and the coalescence for p, d, t, and ^{3}He ejectiles with an additional contribution of the intermediate mass source for ^{4}He particles. The ratio of these cross sections to the total cross sections, which contain also the contribution of the compound nucleus mechanism, is shown in Fig. 12. The compound nucleus cross sections were evaluated by means of the INCL4.3 plus GEM2 programs and were scaled by factors found from the fit to the proton spectra (0.63, 0.69, and 0.73 for beam energies of 1.2, 1.9, and 2.5 GeV, respectively). As can be seen from the figure, the contribution of nonequilibrium processes is very large for all energies. It has the largest values (over 80%) for ^{3}He and for protons. For deuterons and tritons this contribution is about 70%, whereas for α particles it is the smallest, but still quite large (40%–50% depending on the beam energy). The important conclusion is that the energy dependence of the relative contribution of nonequilibrium processes is very weak with the exception of the α particles, where this relative contribution increases by 20% from the lowest beam energy to the highest one. Such an almost constant value of the relative contribution of nonequilibrium processes seems to be rather unexpected in view of strong increase of the total production cross sections in the broad range of the beam energies studied. However, it may be explained by the fact that the cross sections of both equilibrium and nonequilibrium processes increase with energy in a similar manner.

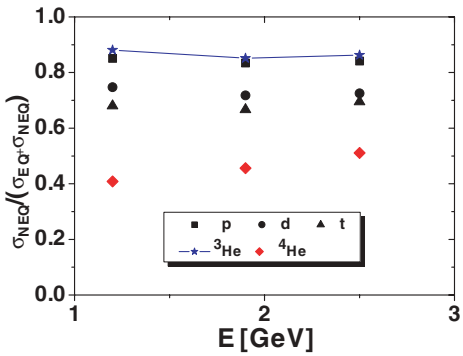

FIG. 12. (Color online) The ratio of the sum of cross sections for nonequilibrium processes to the total cross sections, which additionally contain the compound nucleus contribution described in the text.

V. SUMMARY AND CONCLUSIONS

Double differential cross sections $d^2\sigma/d\Omega dE$ were measured for $p, d, t,^{3,4,6}$He, ^{6,7,8,9}Li, ^{7,9,10}Be, and ^{10,11,12}B produced in collisions of 1.2- and 1.9-GeV protons with a Au target. It was found that the spectra measured at 16°, 20°, 35°, 50°, 65°, 80°, and 100° in the present experiment as well as such data obtained at 2.5-GeV beam energy [1] are very similar, indicating a large contribution of nonequilibrium processes. The data for IMFs were analyzed in the framework of a phenomenological model of two moving sources emitting the ejectiles isotropically in their rest frame. The slow source simulated the evaporation of particles from the equilibrated remnant of the intranuclear cascade of nucleon-nucleon collisions whereas the fast source was responsible for the description of the nonequilibrium processes. A very good reproduction of all cross sections was achieved with parameters smoothly varying with the beam energy and the mass of the ejectiles. It was found that the IMF cross sections corresponding to both sources increase with energy and the relative contribution of the nonequilibrium processes varies from (27 ± 3)% at 1.2-GeV beam energy to (44 ± 5)% at 2.5-GeV beam energy. This is shown in Fig. 3 and discussed in the text.

The LCPs data were analyzed by means of the microscopic model that takes into consideration the intranuclear cascade of nucleon-nucleon collisions, coalescence of the nucleons escaping from the nucleus after the cascade, and the evaporation of particles from the equilibrated, excited residuum of the target nucleus. The calculations were performed by using the INCL4.3 computer program of Boudard *et al.* [7] for the intranuclear cascade and coalescence processes and by using the GEM2 computer program of Furihata [8,9] for evaporation. It should be emphasized that free parameters of both models have *not* been fitted to our experimental data, but original values of the parameters recommended by the authors, respectively, have been used. The cross sections resulting from the model calculations were significantly smaller than the experimental data for the emission of protons with energies larger than ∼30 MeV whereas the evaporation contribution, which dominates the smaller energy range of the spectra, overestimates the data. The discrepancy increases with increasing beam energy and with decreasing emission angle with respect to the incident proton.

It was assumed that an additional contribution to the microscopic model cross sections has to be added to account for the observed discrepancies in the description of proton data.

The isotropic emission of particles from a fireball moving forward (i.e., in the direction parallel to the beam) leads to desirable energy and angular distributions. Thus, this process has been taken into consideration for improving the proton data description. Parameters of the fireball were treated as free parameters. The magnitude of the contribution from the microscopic model was allowed to be scaled down for two reasons: (i) In the intranuclear cascade model it is assumed that *each* proton bombarding the nucleus initiates the cascade of nucleon-nucleon collisions, and thus the fireball process, which consists in creation of a correlated group of nucleons emitted in the forward direction, is completely neglected, and (ii) the magnitude of the coalescence process may be modified by variation of the conditions that determine whether nucleons form a cluster or move independently.

An excellent description of the proton spectra was achieved for all emission angles and for all beam energies with the parameters of the fireball varying smoothly with the beam energy. Furthermore, the factor used to scale down the contribution from the intranuclear cascade modified by coalescence and the contribution of the evaporation was almost energy independent: 0.63, 0.69, and 0.73 for beam energies of 1.2, 1.9, and 2.5 GeV, respectively.

The spectra of other LCPs were analyzed in the same manner; that is, the microscopic model contribution (coalescence and evaporation cross sections) was multiplied by the same factor that was used for the proton channel and parameters of the fireball were fitted independently for each ejectile and each beam energy. An excellent description of all data has been obtained with smoothly varying parameters of the fireball. The data for the ^{4}He channel still need inclusion of the contribution from another slow moving source. Except for ^{3}He, the contribution of the fireball mechanism to the nonequilibrium processes is quite significant for all light charged particles (20%–60%, depending on the particles and beam energy). The magnitude of the fireball contribution increases almost exponentially with the beam energy.

A rather astonishing result of the present investigation—namely, that the relative contribution of all nonequilibrium processes to the total cross sections (40%–80%, depending on the particles) remains almost energy independent for all light charged particles—is caused by presence of similar energy dependence for both equilibrium and nonequilibrium processes in the energy range studied. Such a weak energy dependence of the relative contribution of nonequilibrium processes was also found for production of intermediate mass fragments.

The comparison of parameters of moving sources used in the description of IMF and LCP data at three proton energies (1.2, 1.9, and 2.5 GeV) confirms our hypothesis postulated in Ref. [1], which claims that the proton impinging on the Au target interacts with a group of nucleons lying on its straight path through the nucleus and leads to emission of a fireball consisting of several nucleons. The excited remnant nucleus may decay into two prefragments, which manifest themselves as moving sources of LCPs and IMFs, whereas the fireball emits only neutrons and LCPs. It was found in the present analysis that the parameters of the fireball fitted to the spectra of tritons, ^{3}He, and α particles are very similar to the parameters of the light source emitting IMFs. Therefore, it seems that the genuine fireball contributes mainly to the emission of protons and deuterons and, thus, it consists of 3 to 4 nucleons. Then the lighter prefragment (of mass $\sim$19 nucleons), appearing as a result of the decay of the excited remnant, is responsible for the emission of tritons, ^{3}He, and α particles. The spectra of α particles show also a large contribution originating from the larger prefragment (i.e., from the emission of a slow source responsible for the IMF production).

These findings are in agreement with observations made for hadron production in high-energy (of order of 50–200 GeV) proton-nucleus collisions [11–13] where the reaction does not proceed on the total nucleus of mass A but the bombarding proton interacts with the *effective target* consisting of several nucleons ($\sim 0.7A^{0.31}$) [12]. For the Au target such an effective target would have a mass of 3.6 nucleons, which fits well with the estimated mass of the fireball of the present study and justifies an identification of the fireball with the effective target. Furthermore, the deep spallation process of the production of ^{149}Tb, studied by Winsberg *et al.* [14] in p + Au collisions at energies of 1–300 GeV, was also explained by Cumming [15] by assuming an effective target with a mass of (3.1 ± 0.4) nucleons for proton energies greater than $\sim$2 GeV. This mass again agrees with the fireball mass found in our investigations and confirms the proposed interpretation of the fireball.

It is worth pointing out that the observation of the effective target was also reported in the production of heavy fragments in p + U collisions at proton energies of 11.5 GeV (A = 140–210) [16], at 3–11.5 GeV (A = 131) [17], and in production of lighter fragments at 11.5–400 GeV (^{44}Sc-^{48}Sc) [18], as well as IMFs (with Z = 3–14) in p + Xe collisions at 1–19 GeV [19].

The presence of heavier sources accompanying the fireball and the mechanism of their creation was predicted and discussed in Refs. [2,20–22] as a result of "cleveage" of the excited remnant nucleus into two excited prefragments after the fireball emission. In our analysis these heavier prefragments manifest themselves as two sources emitting IMFs as well as tritons, ^{3}He, and α particles. Their contribution to proton and deuteron spectra is not pronounced; thus it seems that the proton and deuteron spectra are dominated by the emission from the fireball (large ejectile energies) and by the evaporation from a heavy target residuum (small ejectile energies).

In summary, our investigations lead to a consistent picture of the reaction mechanism responsible for nonequilibrium processes, in which the proton impinging on the target can either initiate a cascade of binary nucleon-nucleon collisions accompanied by surface coalescence of nucleons into LCPs or interact coherently with a group of nucleons leading to the emission of three excited groups of nucleons: the fireball and two heavier prefragments with different masses. All three excited groups of nucleons are sources of ejectiles. The present investigation shows that the presence of the effective target and, as a consequence, the fast breakup mechanism, manifests itself at proton beam energies of 1.2–2.5 GeV, lower than those from previous studies quoted here.

The important conclusion of the present study is that for a good description of the double differential cross sections for all LCPs it is necessary to assume competition of two mechanisms of the nonequilibrium processes: coalescence of nucleons escaping from the nucleus after an intranuclear cascade of nucleon-nucleon collisions and isotropic emission of LCPs from the fast source—fireball—moving forward along the beam direction. A need to introduce the presence of the fireball contribution seems to indicate that the lack of correlation between nucleons, inherent in intranuclear cascade models, leads to an oversimplified microscopic description of the reaction mechanism. Thus, the realistic microscopic model has to take this effect into consideration.

ACKNOWLEDGMENTS

We acknowledge gratefully the fruitful discussions on the coalescence mechanism with A. Boudard, J. Cugnon, and S. Leray as well as their providing us with the new version of the INCL4.3 computer program. The technical support of A. Heczko, W. Migdał, and N. Paul in preparation of the experimental apparatus is greatly appreciated. This work was supported by the European Commission through the European Community-Research Infrastructure Activity under the FP6 "Structuring the European Research Area" programme (CARE-BENE, Contract No. RII3-CT-2003-506395, and Hadron Physics, Contract No. RII3-CT-2004-506078) as well as the FP6 IP-EUROTRANS FI6W-CT-2004-516520.

[1] A. Bubak *et al*., Phys. Rev. C **76**, 014618 (2007).
[2] J. Aichelin, J. Hüfner, and R. Ibarra, Phys. Rev. C **30**, 107 (1984).
[3] G. D. Westfall, J. Gosset, P. J. Johansen, A. M. Poskanzer, W. G. Meyer, H. H. Gutbrot, A. Sandoval, and R. Stock, Phys. Rev. Lett. **37**, 1202 (1976).
[4] R. Barna *et al*., Nucl. Instrum. Methods Phys. Res. A **519**, 610 (2004).
[5] A. Boudard, J. Cugnon, S. Leray, and C. Volant, Phys. Rev. C **66**, 044615 (2002).
[6] A. Letourneau *et al*., Nucl. Phys. **A712**, 133 (2002).
[7] A. Boudard, J. Cugnon, S. Leray, and C. Volant, Nucl. Phys. **A740**, 195 (2004).
[8] S. Furihata, Nucl. Instrum. Methods Phys. Res. B **71**, 251 (2000).
[9] S. Furihata and T. Nakamura, J. Nucl. Sci. Technol. Suppl. **2**, 758 (2002); Proceedings of the International Conference on Nuclear Data for Science and Technology October 7–12, 2001, Tsukuba, Ibaraki, Japan; http://www.ndc.tokai-sc.jaea.go.jp/nd2001/proc/pdf/1_0758.pdf.
[10] G. D. Westfall, R. G. Sextro, A. M. Poskanzer, A. M. Zebelman, G. W. Butler, and E. K. Hyde, Phys. Rev. C **17**, 1368 (1978).
[11] G. Berlad, A. Dar, and G. Eilam, Phys. Rev. D **13**, 161 (1976).
[12] C. Halliwell, J. E. Elias, W. Busza, D. Luckey, L. Votta, and C. Young, Phys. Rev. Lett. **39**, 1499 (1977).
[13] T.-C. Meng and E. Moeller, Phys. Rev. Lett. **41**, 1352 (1978).
[14] L. Winsberg, M. W. Weisfield, and D. Henderson, Phys. Rev. C **13**, 279 (1976).
[15] J. B. Cumming, Phys. Rev. Lett. **44**, 17 (1980).
[16] B. D. Wilkins, S. B. Kaufman, E. P. Steinberg, J. A. Urbon, and D. J. Henderson, Phys. Rev. Lett. **43**, 1080 (1979).
[17] S. Biswas and N. T. Porile, Phys. Rev. C **20**, 1467 (1979).
[18] D. R. Fortney and N. T. Porile, Phys. Rev. C **21**, 2511 (1980).
[19] N. T. Porile, A. J. Bujak, D. D. Carmony, Y. H. Chung, L. J. Gutay, A. S. Hirsch, M. Mahi, G. L. Paderewski, T. C. Sangster, R. P. Scharenberg, and B. C. Stringfellow, Phys. Rev. C **39**, 1914 (1989).
[20] M. A. Cirit and F. Yazici, Phys. Rev. C **23**, 2627 (1981).
[21] S. Bohrmann, J. Huefner, and M. C. Nemes, Phys. Lett. **B120**, 59 (1983).
[22] J. Hüfner and H. M. Sommermann, Phys. Rev. C **27**, 2090 (1983).